Supporting Information

Nanostructured Liquid-Crystalline Polymer Films for Ionic Actuators: Self-Assembly of Photopolymerizable Ionic Itaconate with an Ionic Liquid

Che-Hao Wu[a,b] and Masafumi Yoshio*[,a,b]

---

[a] *Research Center for Macromolecules & Biomaterials, National Institute for Materials Science, 1–2–1 Sengen, Tsukuba, Ibaraki 305–0047, Japan*

[b] *Graduate School of Chemical Sciences and Engineering, Hokkaido University, Kita 13, Nishi 8, Kita–ku, Sapporo, Hokkaido 060–8628, Japan*

* E–mail: YOSHIO.Masafumi@nims.go.jp

Captions

1. General procedures and materials.

General procedures. All ^{1}H–NMR and ^{13}C–NMR spectra were recorded on a JEOL ECZ400S spectrometer at 400 MHz and 100 MHz for solutions in $CDCl_3$, respectively. The chemical shifts (δ) are quoted in ppm using the $CDCl_3$ solvent peak as internal reference (δ = 7.26 for ^{1}H–NMR spectra, and δ = 77.16 for ^{13}C–NMR spectra). Matrix–assisted laser desorption/ionization time–of–flight mass spectrometry (MALDI TOF–MS) measurements were carried out with a Shimadzu AXIMA–CFR Plus. Dithranol was used as a matrix. Fourier–transform infrared spectroscopy (FTIR) spectra were taken with a BRUKER FT–IR ALPHA II spectrometer equipped with a single reflection diamond ATR module. Elemental analysis for C, H and N was carried out by using an ELEMENTAR vario EL cube.

Materials. Itaconic anhydride (>95%), 1-Dodecanol (>99%), 4-Dimethylaminopyridine (DMAP, >99%), N,N-dicyclohexylcarbodiimide (DCC, >98%), 1-Ethyl-3-methylimidazolium tetrafluoroborate (**IL**, >99%), 1-(2-hydroxyethyl)-3-methylimidazolium tetrafluoroborate (>98%) were purchased from Tokyo chemical industry. Ethylene glycol were purchased from KANTO CHEMICAL. Poly(3,4-ethylenedioxythiophene) polystyrene sulfonate PEDOT:PSS (Clevios™ PH1000) was purchased from Heraeus. 2,2-Dimethoxy-2-phenylacetophenone as a photo–initiator was purchased from Sigma–Aldrich. All the chemicals were used directly without further purification.

2. Synthesis procedure.

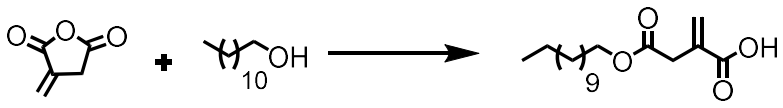

2

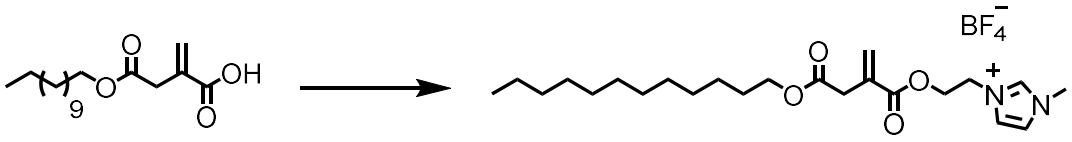

2 **1**

Scheme S1 Synthetic routes of ionic molecule **1**.

Synthesis of compound 2

2

The itaconic anhydride (1 g, 8.92 mmol) was mixed with 1-Dodecanol (2 mL, 8.92 mmol) in a Schlenk flask with stirring. The mixture solution was kept at 100ºC and trace by TLC plate. After the reaction completed, the hot hexane was used to wash the reaction mixture and the crude product was precipitated. The crude product was recrystallized from ethanol to give compound **2** as white crystal. (Yield: 75%)

^{1}H–NMR (400 MHz, $CDCl_3$, δ = ppm): 0.861–0.895 (m, 3H), 1.25 (m, 18H), 1.58–1.63 (m, 2H), 3.33 (s, 2H), 4.07–4.11 (td, 2H), 5.82 (s, 1H), 6.46(s, 1H).

Synthesis of ionic molecule 1

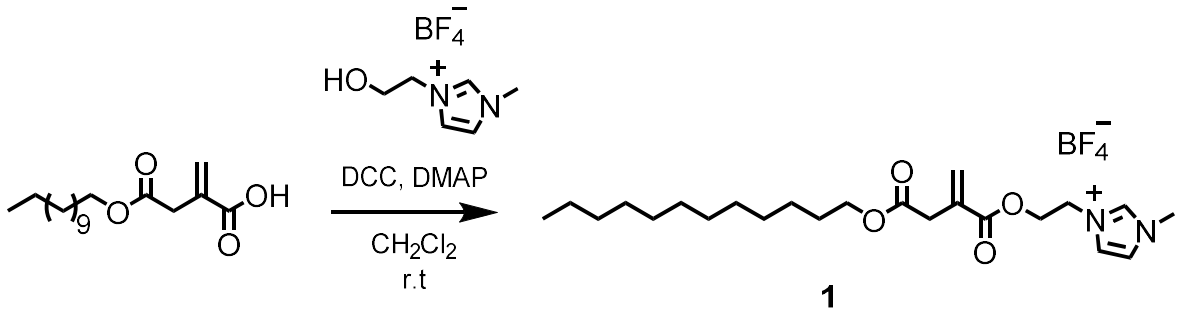

Compound **2** (1 g, 3.35 mmol), *N,N*-dicyclohexylcarbodiimide (DCC; 0.83 g, 4 mmol), 4-dimethylaminopyridine (DMAP; 0.02 g, 0.17 mmol) and 15 mL of DCM were mixed in a Schlenk flask with stirring and purged with argon for 30 minutes in an ice bath. Then, 1-(2-hydroxyethyl)-3-methylimidazolium tetrafluoroborate (0.64 mL, 4 mmol) were added dropwise into the mixture solution by using an addition funnel. The reaction was warmed to room temperature and stirred for 48 hours. The reaction mixture was diluted with DCM and extracted with water three times. The organic phase was collected and dried with $MgSO_4$. After evaporating the solvent, the crude product was purified by column chromatography (eluent: gradient from chloroform : methanol = 100/0 to 90/10 v/v) to give compound **1** as a white liquid crystal. (Yield: 53%)

^{1}H–NMR (400 MHz, $CDCl_3$, δ = ppm): 0.86–0.89 (t, 3H), 1.26 (m, 18H), 1.60–1.65 (m, 2H), 1.85–1.93 (m, 4H), 3.33 (s, 2H), 3.96 (s, 3H), 4.03–4.07 (t, 2H), 4.56 (s, 4H), 5.75 (s, 1H), 6.30 (s, 1H), 7.24 (s, 1H), 7.48 (s, 1H), 8.89 (s, 1H).

^{13}C–NMR (100 MHz, $CDCl_3$, δ = ppm): 14.21, 22.78, 25.97, 28.62, 29.37, 29.45, 29.63, 29.70, 29.74, 29.75, 32.01, 36.42, 37.71, 48.81, 63.07, 65.45, 123.07, 123.72, 129.63, 133.15, 137.11, 165.74, 171.17.

MS (MALDI–TOF): *m/z* calcd. for $C_{23}H_{39}BF_4N_2O_4$, $[M–BF_4]^+$: 407.29; found: 407.03.

Elemental analysis calcd. for $C_{23}H_{39}BF_4N_2O_4$: C, 55.88, H, 7.95, N, 5.67; found: C, 55.99, H, 7.71, N, 5.28.

FT–IR (ATR): *v* = 3163, 3118, 2955, 2922, 2853, 1721, 1637, 1576, 1460, 1427, 1370, 1377, 1315, 1388, 1260, 1170, 1142, 1052, 1031, 966, 940, 846, 817, 758, 723, 703, 652, 624, 599, 548, 522, 479 cm^{-1}.

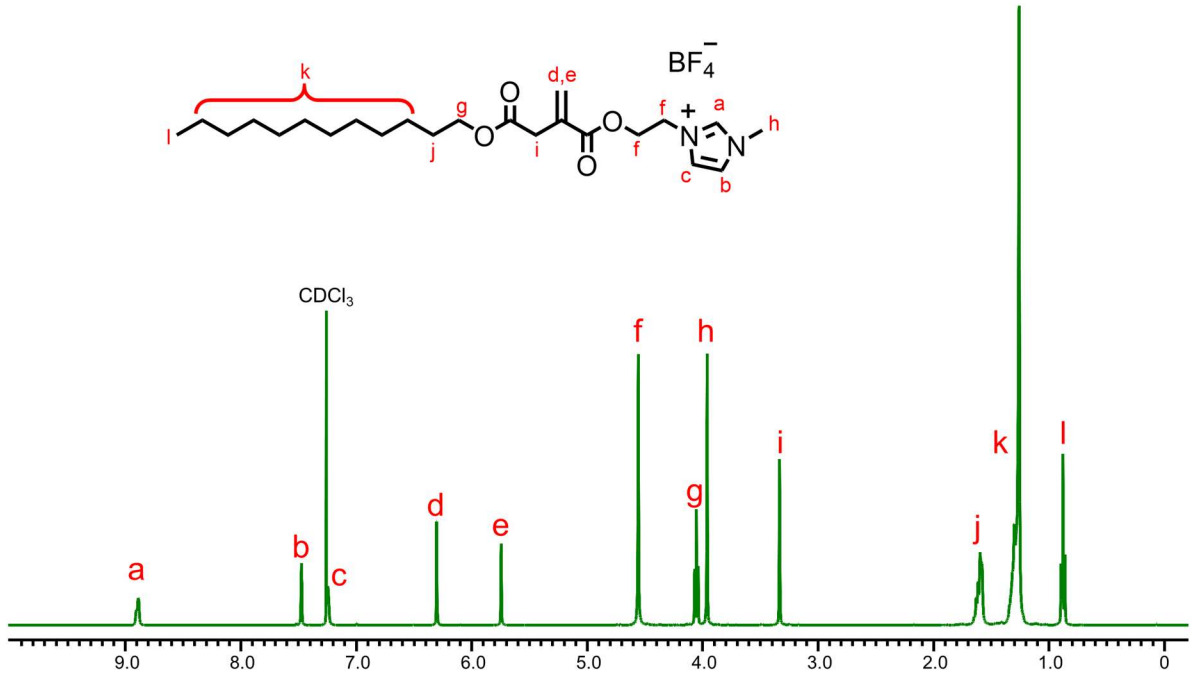

Figure S1 ^{1}H–NMR spectra of **1** (400 MHz, $CDCl_3$).

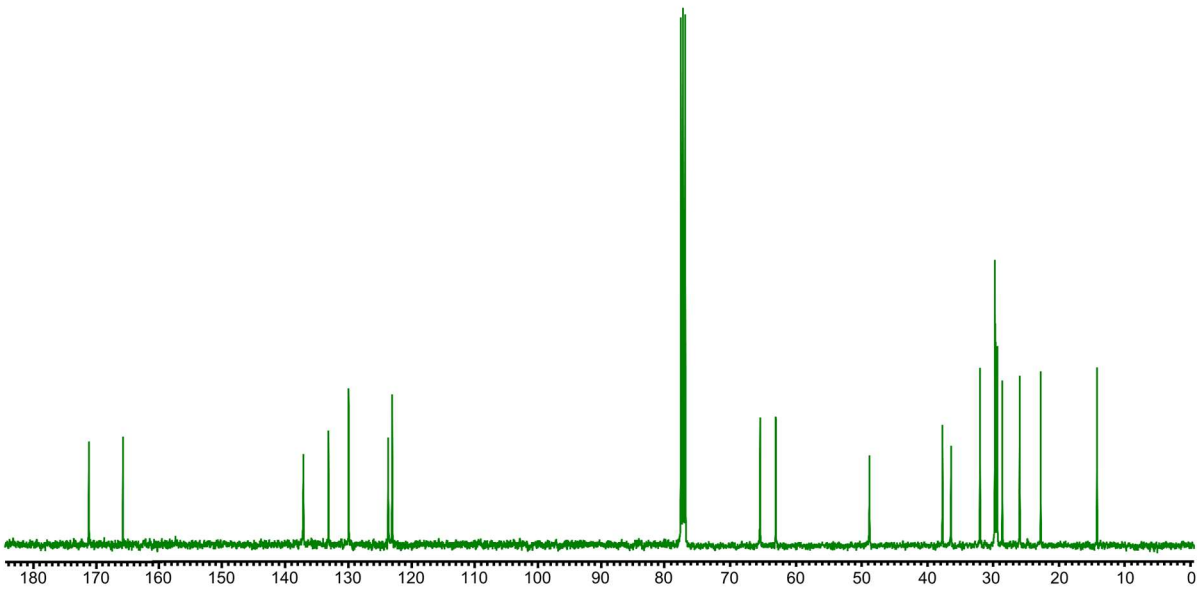

Figure S2 ^{13}C–NMR spectra of **1** (100 MHz, $CDCl_3$).

Fabrication of self–standing PEDOT:PSS electrode films.

A PEDOT:PSS aqueous solution (3 ml) content 10 vol% of ethylene glycol was vigorously stirred for 1 hour. Subsequently, the mixed solution was transferred to ABS plastic tip trays (Nihon Entegris, Inc) and dried at 60 ºC for 4 hours. The resultant gelatinous films containing solvents were carefully peeled off from the substrate and placed on a Teflon plate. After vacuum drying at 120 ºC for 4 hours, the self–standing conductive PEDOT: PSS film with 5 μm ± 1 μm (500–600 S/cm) was obtained. The electrical conductivity of the films was evaluated by four–point method with a Loresta–GX (MCP–T700, Nittoseiko Analytech Co., Ltd.).

Fabrication of ionic liquid–crystalline actuators.

The mixture of ionic molecule **1** and the [EMIM][BF_4] ionic liquid (**IL**) at the 7:3 molar ratio with 2.5 wt% of cross–linker polyethylene glycol diacrylate (PEGDA 400) and 1 wt% of photo–initiator (2,2-dimethoxy-2-phenylacetophenone) were dissolved in a mixed solution of chloroform/methanol (4/1 by volume), and the solvents were removed in a rotary evaporator under light–resistant condition. The monomeric sample **1/IL(30)** containing PEGDA was placed between an untreated cover glass and a glass substrate covered with a polyimide (PI). The sandwiched cell was heated to a temperature at which the sample became the isotropic liquid state and then cooled to room temperature at a rate of 1 ºC/min to form a randomly orientation liquid-crystalline nanostructure. Subsequently, the cell was irradiated with UV light (350 nm, 10 mW/cm^2) for 5 minutes at room temperature. After polymerization, the **P1** film was carefully peeled off from the substrate. The **P1** film was sandwiched between two PEDOT:PSS sheets and pressed. The tri–layered composite was cut into rectangular shape that were used as **P1**–based actuator. The uniaxially parallel aligned nanostructure film, **P1**$_{(//)}$ was prepared from the macroscopically aligned by shearing them parallel to the glass substrate and subsequent polymerization.

3. Characterization of liquid-crystalline structure.

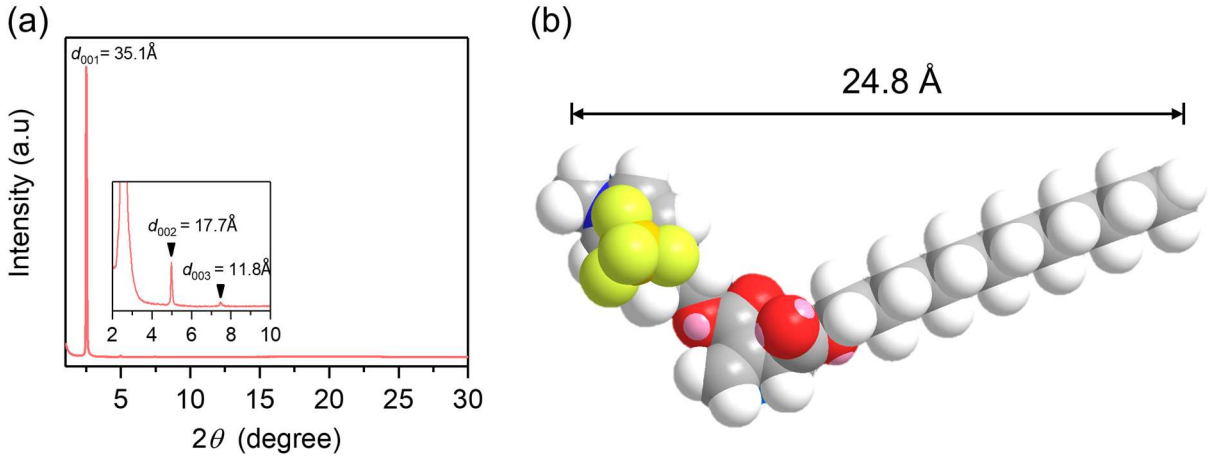

Figure S3 (a) XRD pattern of **1** at room temperature. (b) Molecular structure of **1** calculated by density functional theory.

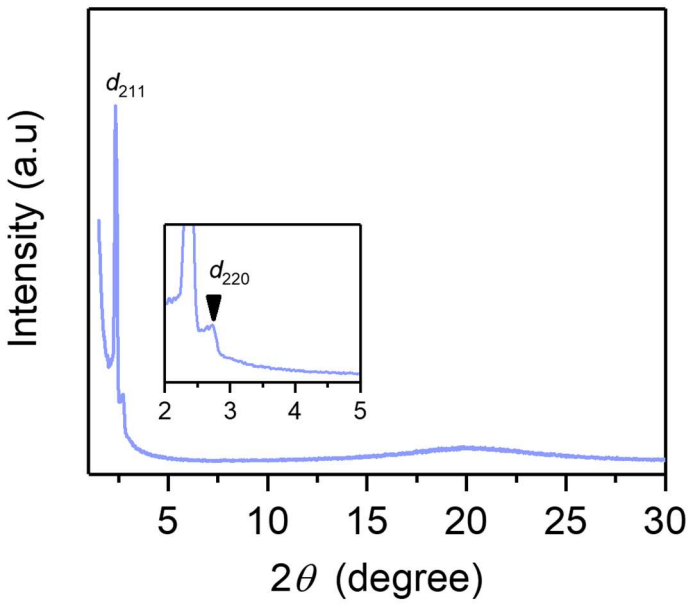

Figure S4 XRD pattern of binary mixture **1/IL(20)** at room temperature.

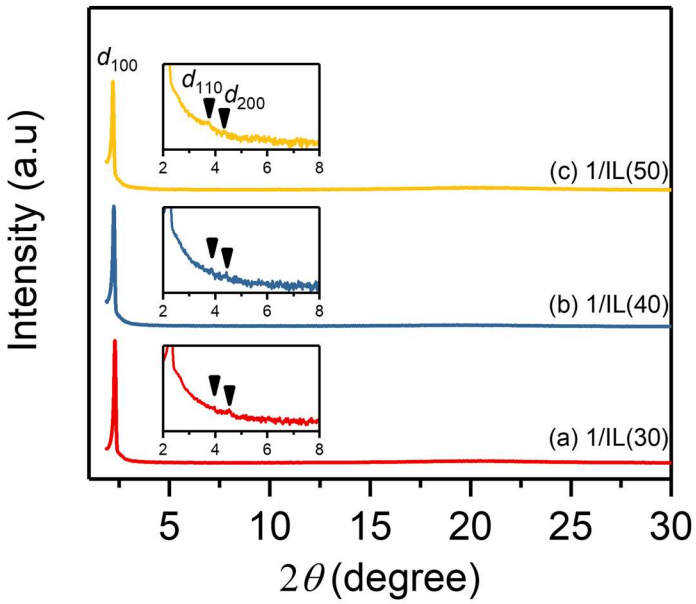

Figure S5 XRD pattern of (a) **1/IL(30)**, (b) **1/IL(40)** and (c) **1/IL(50)** at room temperature.

Table S1 Lattice parameters for the mixtures of **1** and **IL** determined from X-ray diffraction patterns. The measurment was carried out in 25 ºC.

	Structure	Diffraction	Peak (2θ)	*d*–spacing (Å)	Lattice constant, *a* (Å)
		001	2.51	35.17	
1	Sm	002	4.99	17.69	35
		003	7.46	11.84	
		211	2.38	37.09	
1/IL(10)	Cub_{bi}	220	2.73	32.34	91
		–	–	–	
		211	2.35	37.56	
1/IL(20)	Cub_{bi}	220	2.74	32.22	92
		–	–	–	
		100	2.28	38.72	
1/IL(30)	Col_h	110	3.97	22.24	45
		200	4.53	19.49	
		100	2.23	39.59	
1/IL(40)	Col_h	110	3.88	22.75	46
		200	4.43	19.93	
		100	2.19	40.31	
1/IL(50)	Col_h	110	3.76	23.48	47
		200	4.34	20.34	

Table S2 Ionic conductivities (σ) for **1** and **1/IL(x)** at 25 °C and the activation energy (E_a) estimated by the Arrhenius fitting of the temperature–dependent conductivities.

	Structure	Ionic conductivity, σ (S/cm)	Activation energy, E_a (kJ/mol)
1	Sm	1.85×10^{-5}	51.6
1/IL(10)	Cub_{bi}	4.98×10^{-5}	54.3
1/IL(10)	Sm	2.50×10^{-4} (55 °C)	43.8
1/IL(20)	Cub_{bi}	2.06×10^{-4}	37.0
1/IL(30)	Col_h	4.10×10^{-4}	32.1
1/IL(40)	Col_h	5.14×10^{-4}	24.7

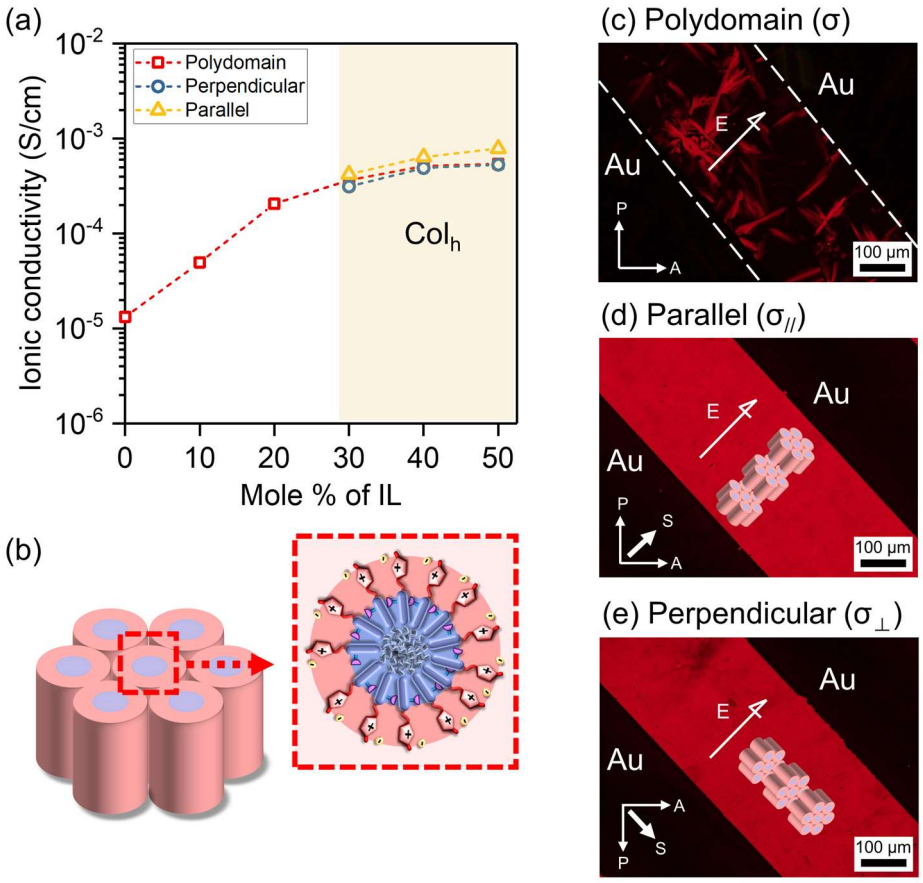

Figure S6 (a) Ionic conductivities of compound **1** as a function of the mole % of **IL**. The yellow area shows the ionic conductivity for the oriented columns (△: parallel and ○: perpendicular to the applied electric field and randomly oriented columns (□). (b) The image illustrated the Col_h LC structure form by the hydrophobic cylinders surrounded by ionic shells. POM images for different orientations of the columns: (c) the columns are randomly oriented between electrodes, (d) the columns are aligned by shearing to the direction of electric field, and (e) the columns are aligned perpendicular to the electric field by shearing. Arrows indicate the directions of the mechanical shear force (*S*), analyzer (*A*), polarizer (*P*), and electric field (*E*).

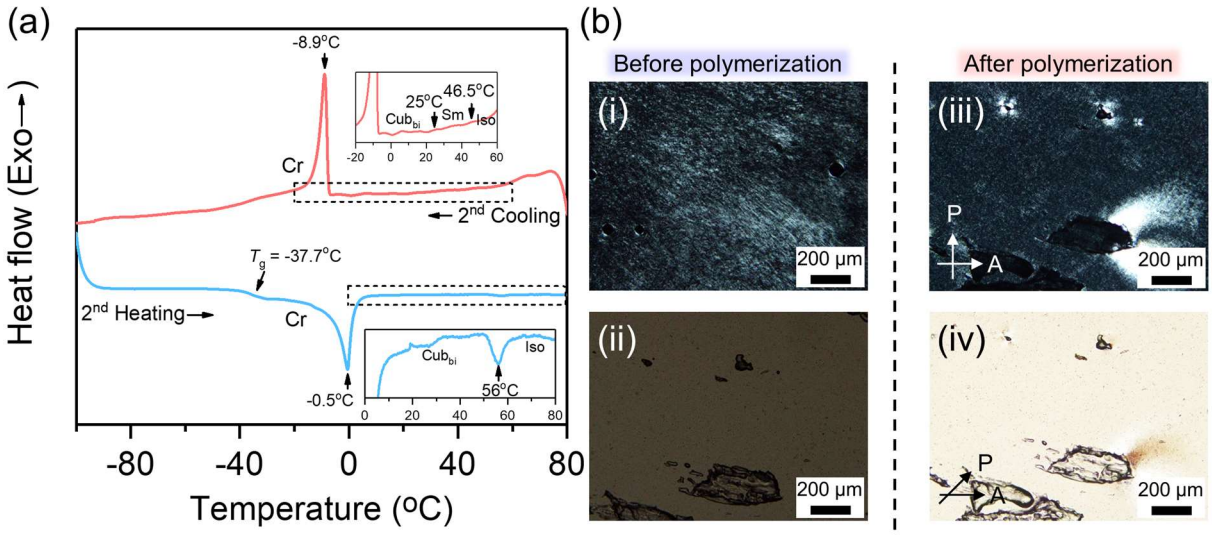

Figure S7 (a) DSC thermograms of **1/IL(20)** containing 1.0 wt% photo-initiator. The inset shows the enlarged view of the selected region of the heating and cooling curves. (b) POM textures of **1/IL(20)** before and after UV irradiation (254 nm; 40 mW; 30 minutes). (i) Oily streak texture observed for **1/IL(20)** in the Sm phase at 30 °C under crossed polarizers, (ii) optically isotropic texture observed for **1/IL(20)** in the Cub_{bi} phase at −1 °C under crossed polarizers, (iii) texture of two-phase coexistence of the Sm and Cub_{bi} phases when a sample obtained by UV irradiation of **1/IL(20)** in the Cub_{bi} phase at −1 °C and heating it to 55 °C, (iv) texture observed for a sample after UV irradiation of **1/IL(20)** in the Cub_{bi} phase at −1 °C. The polarizer is rotated at an angle of 45° to the direction of analyzer. Arrows indicate the directions of the analyzer (*A*), and polarizer (*P*).

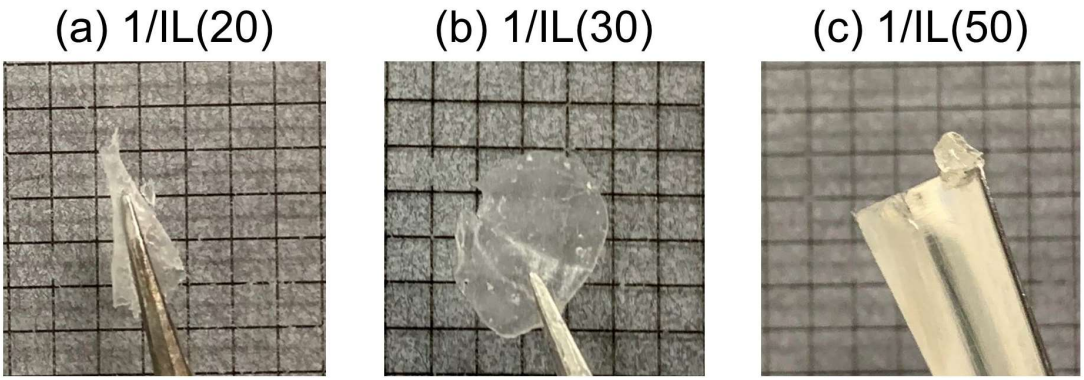

Figure S8 Photographs of the photocured samples of **1/IL(x)**: (a) x = 20, (b) x = 30, (c) x = 50 mol% of **IL**. The grid size is 2 mm.

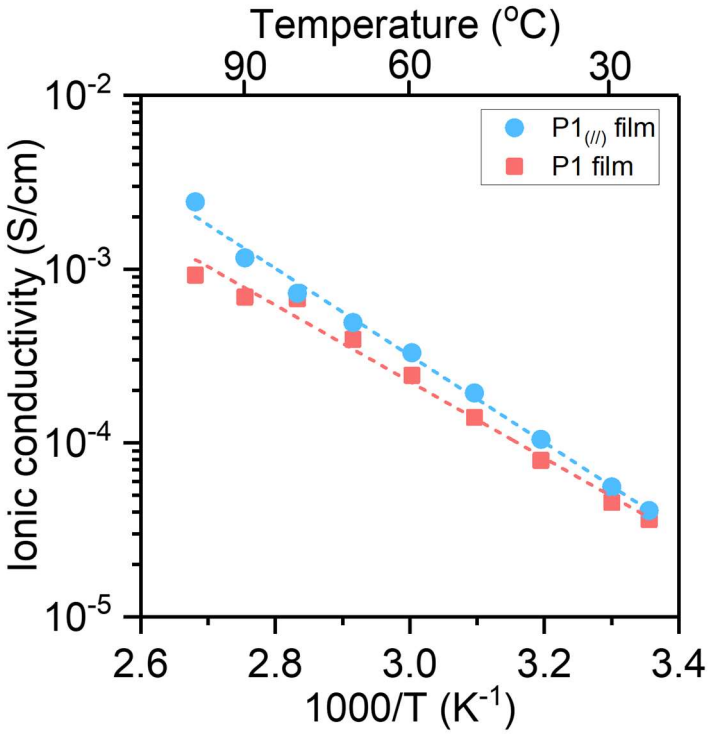

Figure S9 Temperature dependence of ionic conductivity for randomly aligned polymer film (**P1**) and vertical aligned polymer film (**P1**$_{(//)}$).

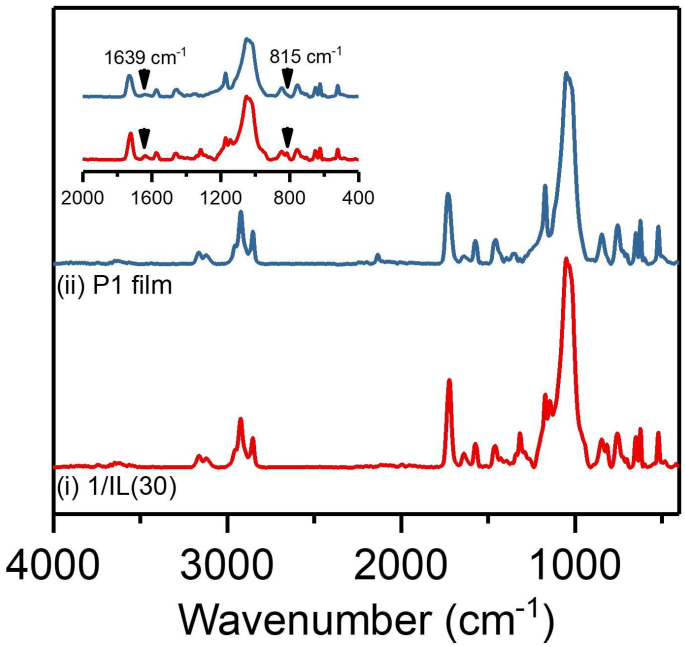

Figure S10 FTIR spectra of (i) **1/IL(30)** containing 2.5 wt% PEGDA 400 and (ii) the polymer film of **P1**. The inset shows the magnified spectra in a wavenumber range of 2000–400 cm^{-1}. The selected characteristic peaks of 1639 and 815 cm^{-1} meant the stretch vibration of acrylate groups.

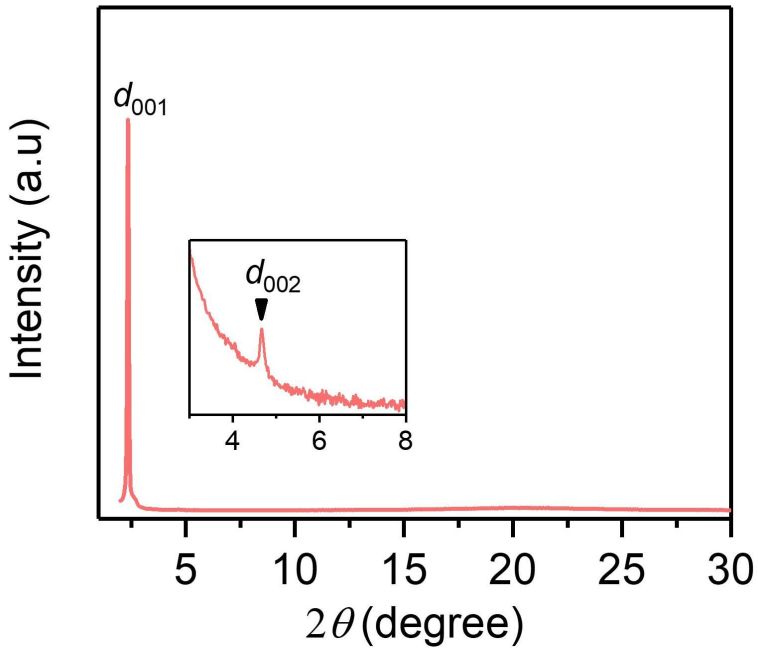

Figure S11 XRD pattern of monomeric mixture **1/IL(30)** containing 2.5wt% PEGDA 400 at 25 °C. The inset indicates the magnified image of the selected region.

Table S3 XRD parameters of **1/IL(30)** containing 2.5 wt% PEGDA 400 and the photocured sample **P1**. The XRD measurments were carried out at 25 °C.

	Structure	Diffraction	Peak (2θ)	*d*–spacing (Å)	Interlayer distance, *a* (Å)
1/IL(30) + 2.5 wt% PEGDA 400	Sm	001	2.35	37.56	38
		002	4.67	18.91	
P1	Sm	001	2.06	42.85	43
		002	4.07	21.69	
		003	6.06	14.57	

4. Characterization of liquid-crystalline membranes and actuators.

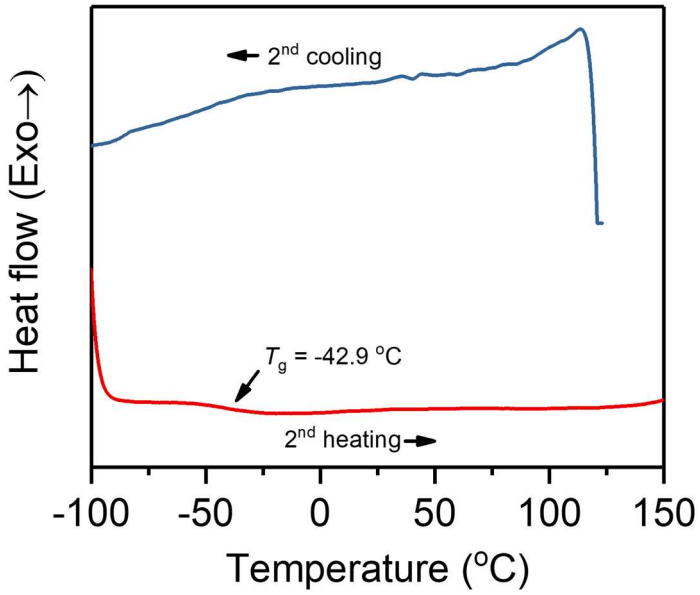

Figure S12 DSC thermograms of **P1** film.

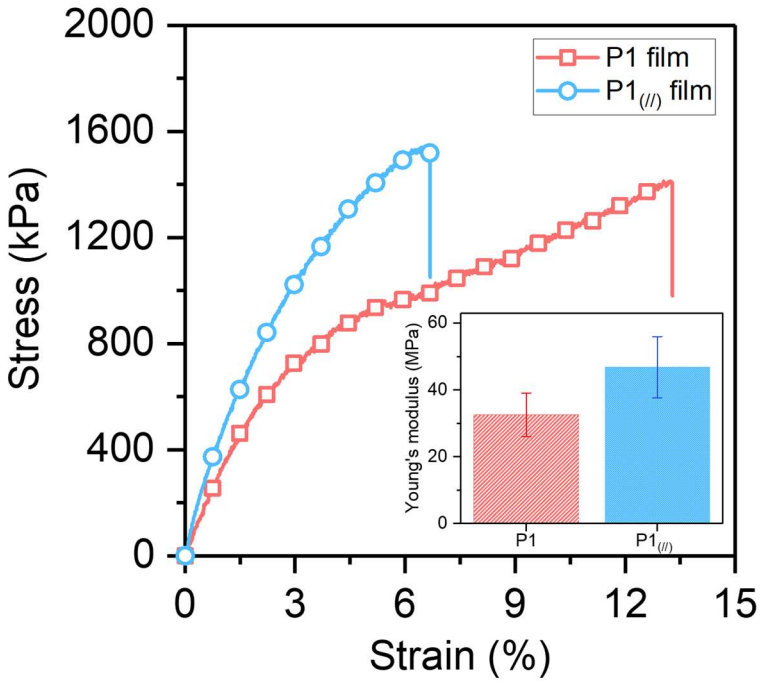

Figure S13 Tensile stress–strain curve of **P1** and **P1**$_{(//)}$ films. The insert shows the corresponding Young's modulus.

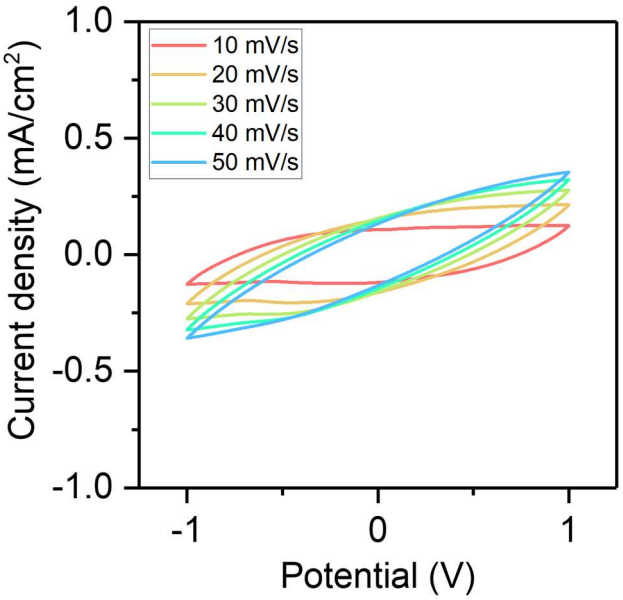

Figure S14 Cyclic voltammograms of **P1**$_{(//)}$–based actuator with the potential range of –1 to 1 V at scan rate of 10 to 50 mV s^{-1}.

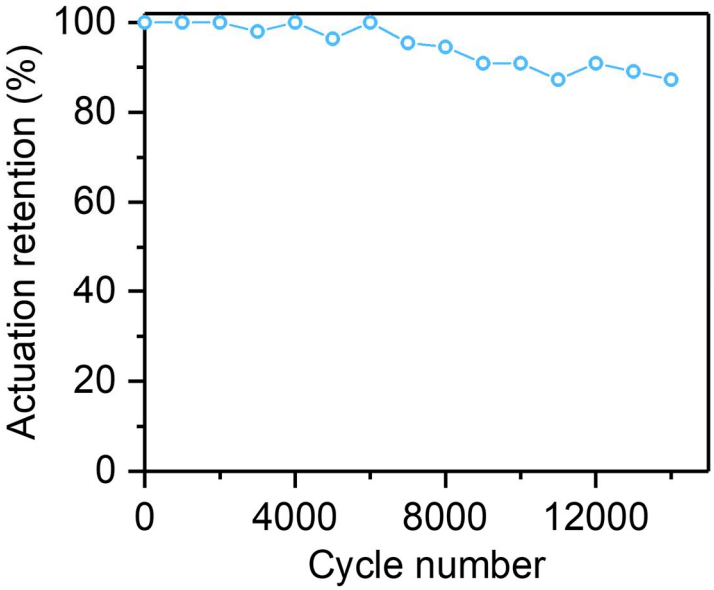

Figure S15 Cyclic stability of **P1**$_{(//)}$–based actuator under 2 V at 1 Hz. The bending strain for each cycle is normalized by the initial strain value.

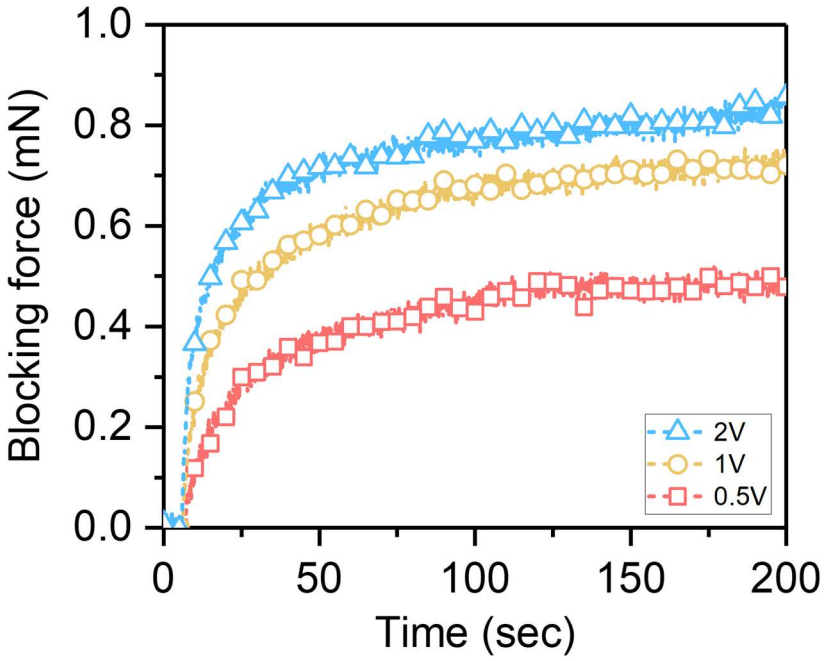

Figure S16 Generating force of **P1**$_{(//)}$–based actuator driven by various DC voltages.

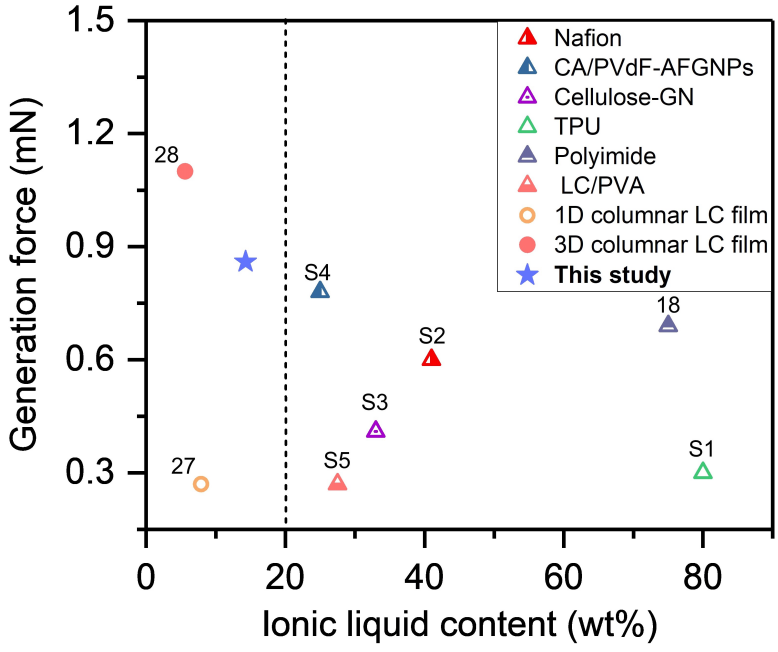

Figure S17 Generation force vs ionic liquid content of **P1**$_{(//)}$–based actuator and other reported ionic actuators.

5. Degradation test of itaconate film.

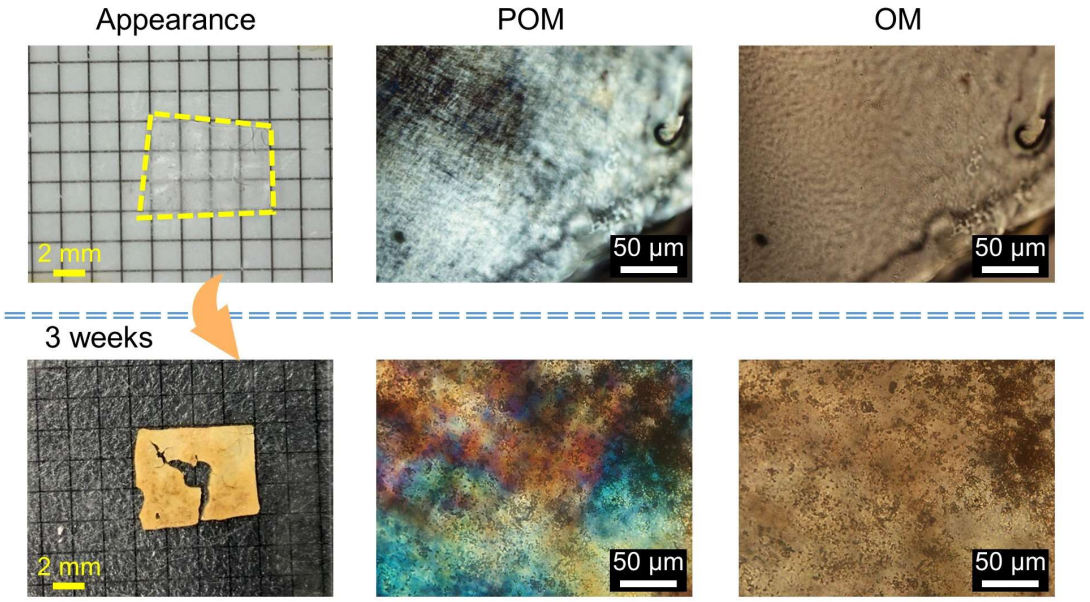

Figure S18 Photographs of **P1** and the POM and optical microscopic images before and after soil incubation for 3 weeks. The initial itaconate film **P1** is transparent. After soil incubation, the film became opaque and had a rough surface topography.

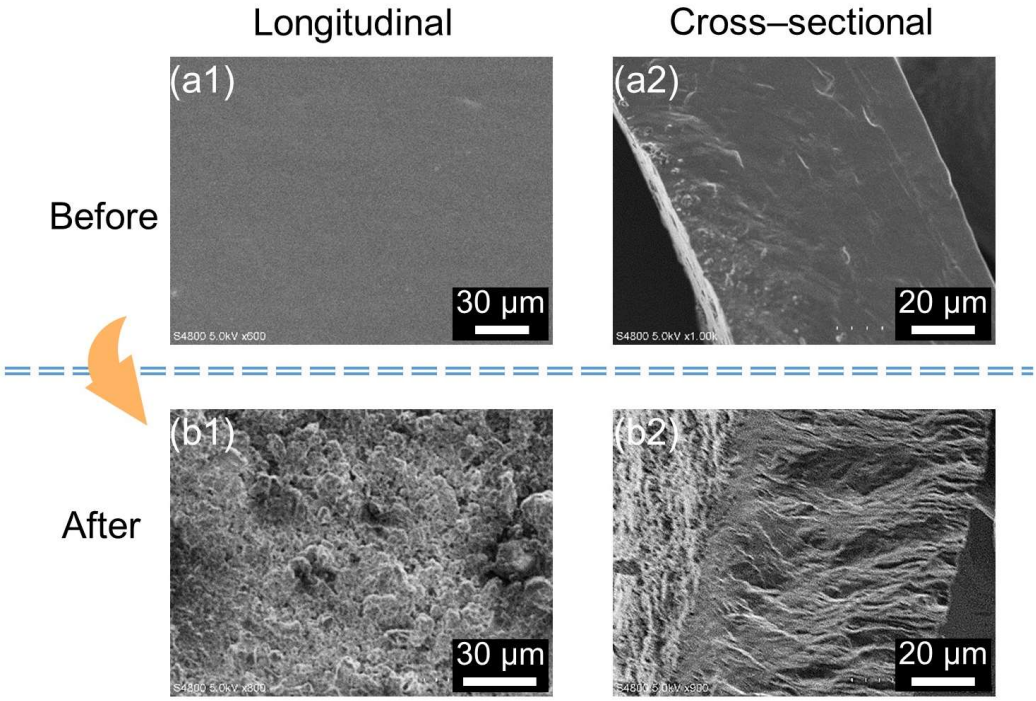

Figure S19 The longitudinal and cross–sectional SEM images of **P1** (a1 and a2) before and (b1 and b2) after soil incubation for 3 weeks.

6. Reference.

S1. S. Y. Kim, C. Kim, H. Cho, H. W. Choi, D. Park, E. Lee, S. Heo, H. Park, D. H. Lee and D. H. Kim, *ACS Appl. Mater. Interfaces*, 2019, **11**, 29350−29359.

S2. M. Kotal, J. Kim, R. Tabassian, S. Roy, V. H. Nguyen, N. Koratkar and I.-K. Oh, *Adv. Funct. Mater.*, 2018, **28**, 1802464.

S3. M. Nan, F. Wang, S. Kim, H. Li, Z. Jin, D. Bang, C. S. Kim, J. O. Park and E. Choi, *Sens. Actuators B*, 2019, **301**, 127127.

S4. M. Nan, D. Bang, S. Zheng, G. Go, B. A. Darmawan, S. Kim, H. Li, C.-S. Kim, A. Hong, F. Wang, J.-O. Park and E. Choi, *Sens. Actuator B*, 2020, **323**, 128709.

S5. S. Cao, J. Aimi and M. Yoshio, *ACS Appl. Mater. Interfaces*, 2022, **14**, 43701−43710.